

Bayesian Nonparametric Vector Autoregressive Models via a Logit Stick-breaking Prior: an Application to Child Obesity

Mario Beraha^{1,2}, Alessandra Guglielmi², Fernando A. Quintana³,
Maria de Iorio⁴, Johan Gunnar Eriksson⁴ and Fabian Yap⁵

¹ Università di Bologna, ² Politecnico di Milano,
³ PUC Santiago de Chile, ⁴ NUS Singapore
and ⁵ KK Women's and Children's Hospital

March 24, 2022

Abstract

Overweight and obesity in adults are known to be associated with risks of metabolic and cardiovascular diseases. Because obesity is an epidemic, increasingly affecting children, it is important to understand if this condition persists from early life to childhood and if different patterns of obesity growth can be detected. Our motivation starts from a study of obesity over time in children from South Eastern Asia. Our main focus is on clustering obesity patterns after adjusting for the effect of baseline information. Specifically, we consider a joint model for height and weight patterns taken every 6 months from birth. We propose a novel model that facilitates clustering by combining a vector autoregressive sampling model with a dependent logit stick-breaking prior. Simulation studies show the superiority of the model to capture patterns, compared to other alternatives. We apply the model to the motivating dataset, and discuss the main features of the detected clusters. We also compare alternative models with ours in terms of predictive performances.

Keywords: clustering, longitudinal profiles, obesity growth patterns, covariate dependent priors.

1 Introduction

Overweight and obesity are defined as abnormal or excessive fat accumulation that may impair health (WHO, 2022). It is well-known that overweight and obesity in adults are associated with risks of metabolic and cardiovascular diseases; see, for instance, Després et al. (2008), Fox et al. (2007) and Pi-Sunyer (2009). Obese individuals are also associated with a more severe course of illness with COVID-19 (Gao et al., 2020).

Obesity is an epidemic, increasingly affecting children. In 2018, 18% of children in the United States were obese and approximately 6% were severely obese (Hales et al., 2018). Prevalence of obesity in children has increased from 4% in 1975 to over 18% in 2016 among children and adolescents aged 5-19 years [WHO, Accessed: 01-06-2021]; see also Cremaschi et al. (2021). Overweight or obesity in childhood is critical as it often persists into adulthood due to both

physiological and behavioural factors, e.g. (i) adults diet based on energy-dense foods that are high in fat and sugars and (ii) adult physical inactivity due to the sedentary nature of many forms of work, changing modes of transportation, and increasing urbanization. Also for childhood obesity, dietary composition and sedentary lifestyle have often been cited as main contributors. Evidence also exists for a significant role of parents' socioeconomic status and maternal prenatal health factors; see Cremaschi et al. (2021).

Research on the origins of health and disease suggests that susceptibility to metabolic disease may originate early in life. Different conditions in maternal uteruses seem to influence metabolic health by altering glucose metabolism and body composition. See Symonds et al. (2013) and Godfrey et al. (2012). Moreover, increased adiposity have been observed in school-age children and infants (Nightingale et al., 2010; Whincup et al., 2005; Yajnik et al., 2002, 2003).

It is therefore important to understand whether obesity persists from early life to childhood and if different types of obesity growth can be detected. For instance, Zhang et al. (2019) show that rates of change in Body Mass Index (BMI) at different childhood ages are differentially associated with adult obesity. Our motivating application is the study of obesity over time in a dataset of children in South Eastern Asia (see Soh et al., 2014), taken every 6 months from birth. In particular, we consider both their height and weight. It is known that obesity might increase the risk of metabolic diseases, and that this risk is higher in Asian populations than in White Caucasian population (Misra and Khurana, 2011). The aim of this manuscript is to cluster children according to obesity growth patterns. Information is available on children as well as mothers. In particular, we focus on clustering the children after adjusting for covariates (of both fixed and time-varying types). We assume a bivariate vector autoregressive (VAR) model for joint responses (height and weight). VAR models may provide a flexible and powerful representation of longitudinal data; see, for instance, Canova and Ciccarelli (2004) and Daniels and Pourahmadi (2002).

We specify a time-dependent Bayesian nonparametric prior on the VAR coefficients to allow for data-driven clustering of the children. More in details, we assume the children-specific VAR coefficients to be independently distributed according to a truncated stick-breaking prior with weights that depend on baseline covariates. This construction induces a prior on the partition of the children in the sample. Moreover, it allows for potentially empty clusters, in which case the *number of clusters* is interpreted as the number of non-empty components in the stick-breaking representation, i.e. components to which at least one observation is assigned.

The dependent stick-breaking prior adopted here can be seen as a finite-dimensional version of the logistic stick-breaking process described in Ren et al. (2011). Covariate dependent random probability constructions include the probit stick-breaking process (Chung and Dunson, 2009; Rodríguez and Dunson, 2011). These Bayesian nonparametric random probability measures stem out from the seminal work by MacEachern (2000) on dependent Dirichlet processes. See a review of this and related models in Quintana et al. (2022). Covariate dependent priors for random partition were first proposed in Müller et al. (2011) and Park and Dunson (2010).

Bayesian nonparametric methods have been successfully applied to VAR models in recent years. See Kalli and Griffin (2018) for such a model applied to single subject data, Billio et al. (2019) and Kundu and Lukemire (2021) for multiple subject data. In Billio et al. (2019) the authors propose a Dirichlet process mixture of normal-Gamma priors on the VAR auto-covariance elements, as a Bayesian-Lasso prior. Kundu and Lukemire (2021) focus on matrix-variate data, providing a class of non-parametric Bayesian VAR models, based on heterogeneous multi-subject data, that enables separate clustering at multiple scales, and result in partially overlapping clusters.

Our contribution includes the design of an efficient Gibbs sampling algorithm to perform

posterior inference, that exploits recent results on logit stick-breaking priors by Rigon and Durante (2021). Note that this random probability measure is represented by a finite random probability with H support points, but, unlike the sparse mixture in Frühwirth-Schnatter and Malsiner-Walli (2019), (i) the weights depend on covariates and (ii) come from a stick-breaking construction, thus implying stochastic dominance of the sequence itself (for a fixed value of the covariate).

Finally, Cremaschi et al. (2021) consider a more complex model in a similar framework, i.e. they provide a joint model for multiple growth markers and metabolic associations, which allows for data-driven clustering of the children and highlights metabolic pathways involved in child obesity. Unlike our approach, they assume a Bayesian joint non-parametric random effect distribution on the parameters characterizing the longitudinal trajectories of obesity and the graph capturing the association between metabolites.

The remainder of this paper is structured as follows. Section 2 describes the motivating application and introduces a preliminary exploratory analysis. In Section 3 we present the finite mixture of VAR models and discuss its main features. Section 4 summarizes the results of three simulation studies carried out to test and compare posterior inference under possible alternative model formulations. Section 5 presents the results from the main application. Section 6 concludes the paper with a discussion. The appendix provides details on the Gibbs sampler algorithm for posterior simulation, and presents further simulations.

2 Child growth dataset

We focus on the analysis of obesity in children from Singapore, particularly on its evolution over time. As mentioned in the Introduction, it is relevant to understand whether obesity persists from early life to childhood. Such information is of particular relevance when designing intervention policy. Section 2.1 introduces the data and explains the main research questions, while Section 2.2 contains a short summary of the exploratory analysis carried out to highlight the main data characteristics.

2.1 Description of the dataset

We consider data from *the Growing Up in Singapore Towards healthy Outcomes* (GUSTO) study, which comprises one of the most carefully phenotyped parent-offspring cohorts with a particular focus on epigenetic observations; see Soh et al. (2014) for description of the recruited women and objectives of the cohort study. The data consist of measurements of child height (or length, depending on the child’s age) in centimeters and weight in kilograms from periodic visits of 1139 children from birth to the age of seven. We consider only visits occurred every 6 months, though during the first year of life, infants were visited every 3 months. More specifically, the response vector $\mathbf{y}_{it} \in \mathbb{R}^2$ is given by the measurements of (*length*, *weight*) up to the 12th month of age ($t = 3$) and (*height*, *weight*) from the 18th month onwards ($t = 4, \dots, 14$). Besides sex of the child, information is available on the mother. However, the original sample includes missing observations. More in details, 77 subjects are discarded from the analysis, because only information on the first visit (i.e. right after birth) is available. Moreover, we discard children with less than two consecutive visits, and with missing baseline covariates. This leads to a final sample size of $N = 766$. Note that we keep children with missing responses, since in Bayesian framework it is straightforward to imputing these as part of the MCMC. To this end, we simulate the missing responses from their full conditional distribution at every iteration of the algorithm. See the MCMC algorithm in Appendix B.

The available baseline covariates in the dataset are:

- *age*, mother’s age: it ranges from 18 to 46 years.
- *parity*: number of previous pregnancies carried to a viable gestation by the mother, ranging from 0 to 5. If parity equals to 0, the child is the first born.
- *OGTT fasting Pw26*: oral glucose tolerance test (OGTT) at 24th-26th week of pregnancy; it varies from 2.9 to 8.7 mg/dL. Mothers are tested after fasting for at least eight hours.
- *OGTT 2hour Pw26*: oral glucose tolerance test at 24th-26th week of pregnancy; it ranges from 2.9 to 15.1 mg/dL. Mothers are tested two hours after having assumed a glucose solution containing a dose of sugar.
- *ppBMI*: pre-pregnancy body mass index of the mother; values in the sample range from 14.6 to 41.3 Kg/m².
- *GA*: gestational age in weeks, i.e. the length of the pregnancy (from 28 to 41.4 in the dataset).
- *sex*: sex of the child.
- Mother’s *ethnicity*: Chinese, Malay or Indian with proportions reflecting those characterising the Singaporean population.
- Mother’s highest *education*: it is a categorical variable with three ordered levels. Level 1 corresponds to no education or primary school, level 2 corresponds either to primary school, GCE (Singapore-Cambridge general certificate of education (O-level)) or ITE NTC (institute of technical education, national technical certificate) and level 3 corresponds to university degree.

The main goal of the analysis is to understand differences among ethnic groups, but we are also interested in assessing the effect of sex, parity and gestational age of the children on the development of obesity (Tint et al., 2016). Sex, age and parity have been reported in the medical literature as associated to neonatal adiposity. Girls are known to have greater adiposity than boys even at birth (Simon et al., 2013; Fields et al., 2009; Rodríguez et al., 2004). Increasing parity is associated with increasing neonatal adiposity in Asians as well as in Western populations (Joshi et al., 2005; Catalano et al., 1995). Gestational age and postnatal age have also been shown to be associated with increasing weight and adiposity (Simon et al., 2013; Catalano et al., 1995). Other important factors relating to the mother are the results of the glucose tolerance test and pre-pregnancy body mass index, since metabolic diseases are heritable, though they do not necessarily lead to obesity (CDS, 2018); see also, for instance, Qasim et al. (2018). Since obesity might also be related to family nutritional habits, we include in the model *education* as proxy for the family socioeconomic status.

In the next subsection we present an exploratory data analysis (EDA), which will drive the choice of interactions between the covariates described above.

2.2 Exploratory data analysis

The three main ethnic groups in Singapore are Chinese, Malay and Indian. Their sample frequencies in the dataset, 56%, 26% and 18%, respectively, are consistent with the overall distribution in the population.

In Figure 1 we plot the sample correlation of the numerical covariates. We find that the largest correlation (equal to 0.42) is between *OGTT fasting* and *OGTT 2h*.

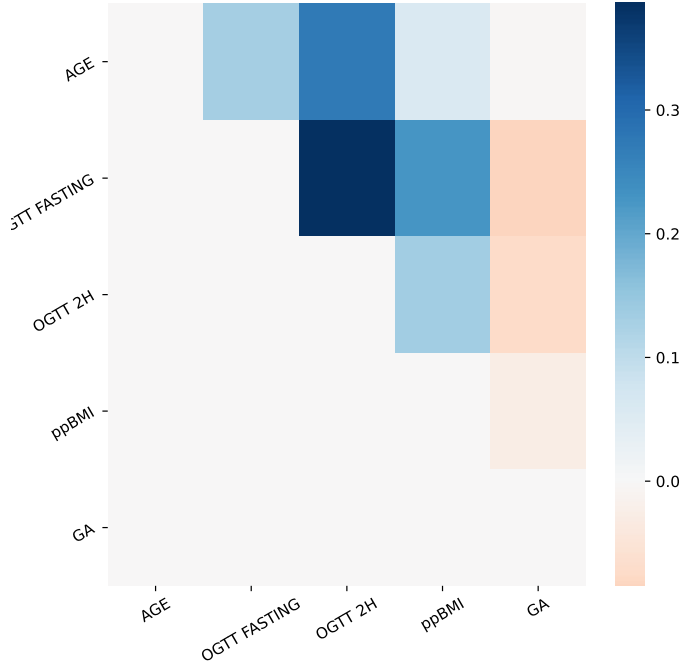


Figure 1: Sample correlation between numerical covariates in Section 2.1

To understand the relationship between categorical and continuous covariates, Figure 2 shows histograms of each continuous covariate, stratified by each categorical covariate level. There appears to be a linear trend between *parity* and *age*, which is to be expected, and also between *parity* and *ppBMI*. Additionally, the distribution of mother’s is concentrated on smaller values for Malay and Indian ethnicity, compared to Chinese women. No other association is detectable between categorical and continuous covariates.

In Appendix A we show the unidimensional scatterplots of the responses (height and weight) at time $t = 0, 1, 2$ versus the continuous covariates, with the goal of identifying effect of these covariates, which are time-homogeneous (recorded at baseline), on the responses (time-varying). For categorical covariates we plot by boxplots of the responses stratified by level. See Figure 12-13 in Appendix A, which display a time-increasing response patterns, though there does not seem to be a clear dependence of weight and height on the covariates.

Figure 3 shows the scatterplots of the children’s height (left) and weight (right) at lag 1, i.e. we plot sample points (y_{it}, y_{it+1}) for all t and all subject i for both responses y . It is to identify two sub-groups in both plots, corresponding to newborns and infants (the group of datapoints on the left bottom corner) and older children. For the latter the autoregressive assumption is very clear, while for the infant group, as expected, the linearity assumption is not strong, though it could be used as first approximation.

As such, we propose a VAR model with lag 1 for the responses. Moreover, we include in the analysis the time-homogeneous covariates z_i and a function of time, $x_{it} = \sqrt{t}$, as time-varying covariate in the model, to account for a global growth trend over time; no other time-varying covariate is available in the dataset. We also consider interaction terms between (i) the mother’s highest education and age, and (ii) ethnicity and sex of the child. Finally, denoting by $X : Y$

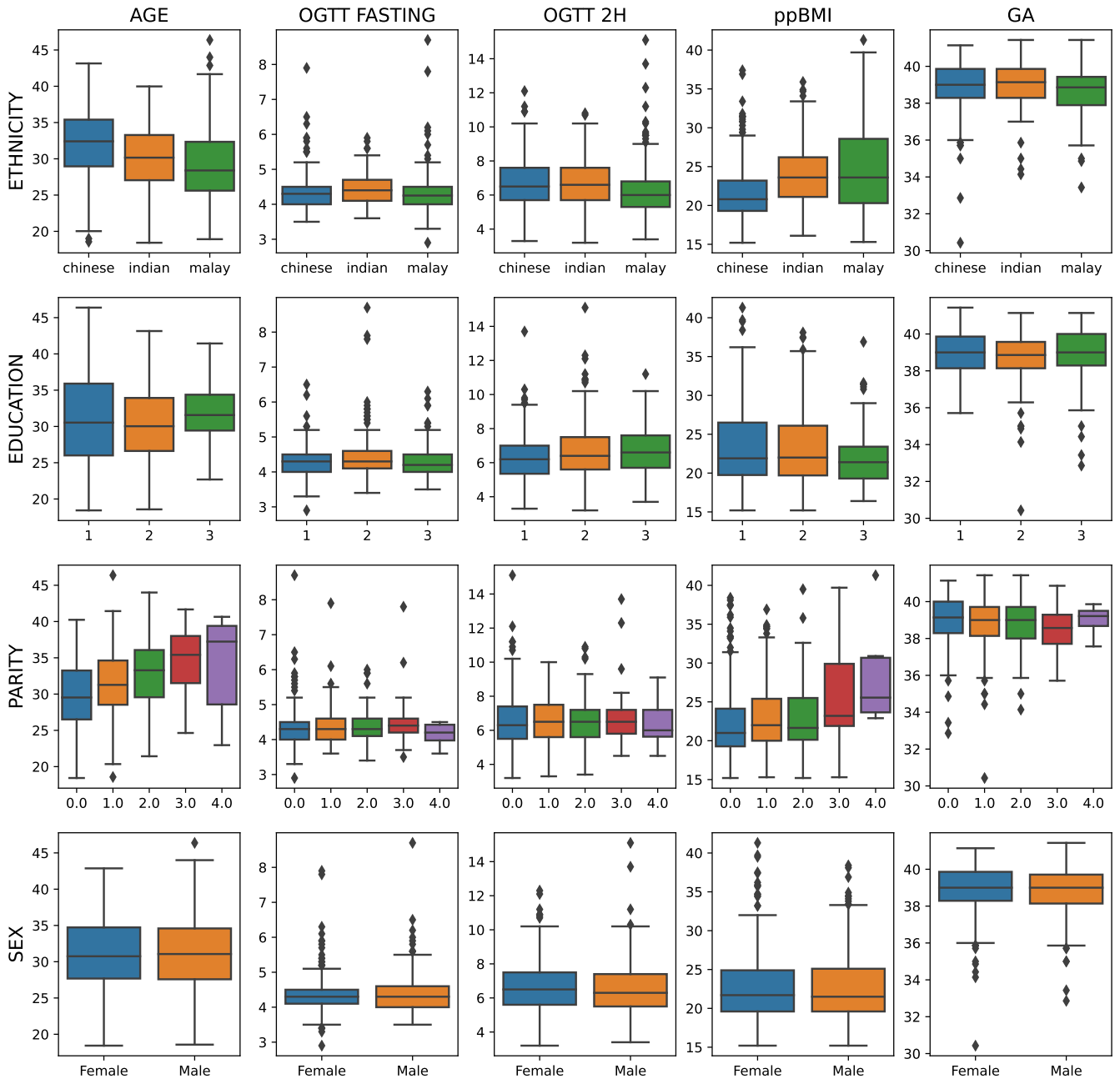


Figure 2: Boxplots of numerical variables (by column) for each level of the categorical variables (by row).

the interaction term between X and Y , we include the following covariates in the model: (1) an intercept, (2) *age*, (3) *parity*, (4) *OGTT fasting Pw26* (in what follows referred to as *OGTT fasting*), (5) *OGTT 2h Pw26* (in what follows referred to as *OGTT 2h*), (6) *ppBMI*, (7) *GA*, (8) *education₁:age* (9) *education₂:age*, (10) *education₃:age*, (11) *parity:age*, (12) *Indian*, an indicator variable, equal to 1 if the mother is Indian and zero otherwise, (13) *Malay* an indicator variable, equal to 1 if the mother is Malay and zero otherwise, (14) *Male:Chinese* indicator variable equal to 1 for a male child born to a Chinese mother, (15) *Male:Indian* indicator variable equal to 1 for a male child born to an Indian mother and (16) *Male:Malay* indicator variable equal to 1 for a male child born to a Malay mother.

The baseline category for the categorical covariates corresponds to a female child born to

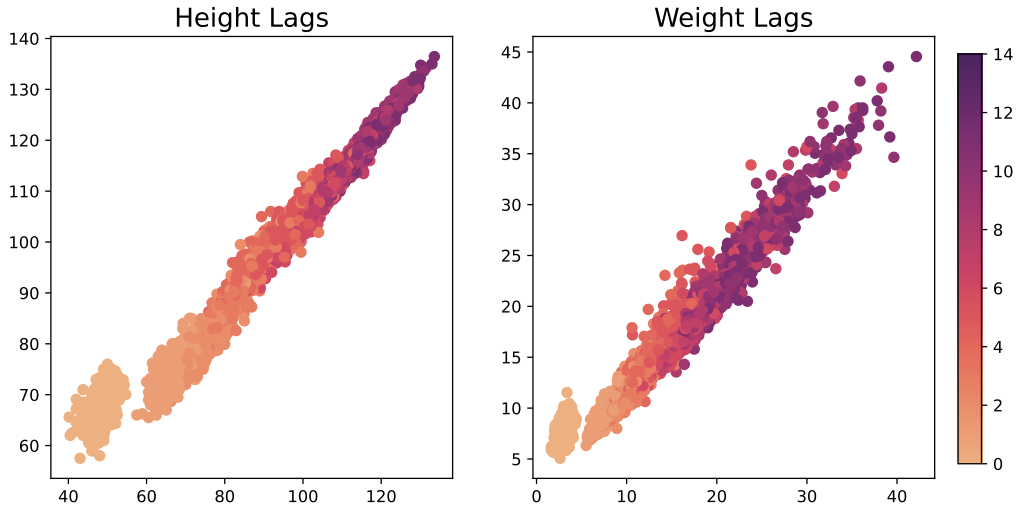


Figure 3: Scatterplots of Singapore children’s height (left) and weight (right) at lag 1, i.e. of the sample points (y_{it}, y_{it+1}) , for $t = 1, \dots, T_i - 1$ and $i = 1, \dots, N$ for response y ; color corresponds to the age in the colorbar

a Chinese mothers. As final pre-processing step, we standardize each numerical covariate at baseline by subtracting their sample mean and dividing by the sample standard deviation.

In summary, the Child Growth dataset contains information on $N = 766$ children, $k = 2$ responses, $p = 1$ time-dependent covariate (that is \sqrt{t}) and a $q = 14$ -dimensional design matrix for time-homogeneous covariates (including intercepts, interactions and dummy variables to represent categorical covariates).

3 The VAR model and the logit stick-breaking prior for the VAR parameters

Our motivating application requires the development of statistical methodology able to describe the evolution of a k -dimensional response vector \mathbf{Y}_{it} for individuals i , $i = 1, \dots, N$ recorded at discrete time points t , $t = 1, \dots, T_i$, accounting for time-varying covariates \mathbf{x}_{it} and time-homogeneous covariates \mathbf{z}_i , measured at the baseline. Motivated by the exploratory analysis in Section 2, we assume:

$$\mathbf{y}_{it} = \Phi_i \mathbf{y}_{it-1} + B \mathbf{x}_{it} + \Gamma \mathbf{z}_i + \boldsymbol{\varepsilon}_{it}, \quad \boldsymbol{\varepsilon}_{it} \stackrel{\text{iid}}{\sim} \mathcal{N}(\mathbf{0}, \Sigma) \quad t = 1, \dots, T_i, \quad i = 1, \dots, N, \quad (1)$$

where $\Phi_i = [\Phi_{ijl}]$ is a $k \times k$ matrix of autoregression coefficients, \mathbf{x}_{it} is a p -dimensional vector of time-varying covariates, \mathbf{z}_i is a q -dimensional vector of time-homogeneous covariates, $B = [b_{jl}]$ and $\Gamma = [\gamma_{jl}]$ are $k \times p$ and $k \times q$ matrices of regression coefficients, respectively. For ease of explanation, we vectorize matrices Φ_i , B and Γ . Specifically, denoting with $(\cdot)^T$ the transpose of a column vector, we introduce the following notation

$$\begin{aligned} \varphi_i &= (\Phi_{i11}, \dots, \Phi_{i1k}, \Phi_{i21}, \dots, \Phi_{i2k}, \dots, \Phi_{ik1}, \dots, \Phi_{ikk})^T \\ \mathbf{b} &= (b_{11}, \dots, b_{1p}, b_{21}, \dots, b_{2p}, \dots, b_{k1}, \dots, b_{kp})^T \\ \boldsymbol{\gamma} &= (\gamma_{11}, \dots, \gamma_{1q}, \gamma_{21}, \dots, \gamma_{2q}, \dots, \gamma_{k1}, \dots, \gamma_{kq})^T, \end{aligned}$$

so that φ_i , \mathbf{b} and $\boldsymbol{\gamma}$ are vectors with k^2 , $k \times p$ and $k \times q$ elements (vectorization of the matrices Φ_i , B , Γ , respectively). We assume $\mathbf{y}_{i0} = \mathbf{0}$, that is, conditionally to the remaining parameters,

\mathbf{y}_{i1} has a Gaussian distribution with mean $B\mathbf{x}_{i1} + \Gamma\mathbf{z}_i$. Alternatively, we could consider the responses at baseline as exogenous. Moreover, different initial distribution could be specified. We assume that a priori (Φ_1, \dots, Φ_N) , \mathbf{b} , $\boldsymbol{\gamma}$ and Σ are independent. As random effect distribution we assume a Bayesian nonparametric prior which depends on the baseline covariates. Specifically, we assume that

$$\Phi_i | z_i \stackrel{\text{iid}}{\sim} \sum_{h=1}^H w_h(\mathbf{z}_i) \delta_{\Phi_{0h}} \quad i = 1, \dots, N. \quad (2)$$

and we impose a stick-breaking construction on the weights w_h . As such, equation (2) defines a truncated stick-breaking prior with H support points $\{\Phi_{0h}\}$ and covariate-dependent weights summing to 1. Similarly to Rigon and Durante (2021), we assume that the weights are generated via a logit stick-breaking construction, that is, $w_1(\mathbf{z}_i) = \nu_1(\mathbf{z}_i)$, and $w_h(\mathbf{z}_i) = \nu_h(\mathbf{z}_i) \prod_{l=1}^{h-1} (1 - \nu_l(\mathbf{z}_i))$ for $h = 1, \dots, H-1$, and $\nu_H(\mathbf{z}_i) = 1$. The dependence on the covariates \mathbf{z}_i is introduced by assuming a logistic model for $\nu_h(\mathbf{z}_i)$:

$$\begin{aligned} \text{logit}(\nu_h(\mathbf{z}_i)) &= \mathbf{z}_i^T \boldsymbol{\alpha}_h, \quad h = 1, \dots, H-1 \\ \boldsymbol{\alpha}_h &\stackrel{\text{iid}}{\sim} \mathcal{N}_q(\boldsymbol{\mu}_\alpha, \Sigma_\alpha), \quad h = 1, \dots, H-1 \end{aligned} \quad (3)$$

An equivalent formulation of (2) can be obtained by introducing auxiliary variables c_i 's (usually referred to as cluster allocation indicators) such that

$$c_i | z_i, \boldsymbol{\alpha} \sim \text{Categorical}(\{1, \dots, H\}; \mathbf{w}(\mathbf{z}_i)),$$

and letting $\Phi_i = \Phi_{0c_i}$. The introduction of the c_i 's allows us to make a fundamental distinction between mixture components and clusters. In the following, we refer to any of the Φ_{0h} 's as a *component*, while we call a *cluster* of observations a (nonempty) set $\{i : c_i = h\}$; see, for instance, Argiento and De Iorio (2019). The marginal prior (2) - (3) is represented by a finite, though large number of parameters, and can be regarded as the truncation of a dependent Bayesian nonparametric prior.

We complete the prior specification with the marginal parametric prior distributions of \mathbf{b} , $\boldsymbol{\gamma}$ and Σ :

$$\mathbf{b} \sim \mathcal{N}_{kp}(\mathbf{0}, \Sigma_B), \quad \boldsymbol{\gamma} \sim \mathcal{N}_{kq}(\mathbf{0}, \Sigma_\Gamma), \quad \Sigma^{-1} \sim \mathcal{W}(\Sigma_0, \nu), \quad (4)$$

where $\mathcal{W}(\Sigma_0, \nu)$ denotes the Wishart distribution with expectation equal to $\nu\Sigma_0$ for $\nu > p - 1$.

To obtain more robust inference, we assume a hierarchical prior for the φ_{0h} 's:

$$\varphi_{0h} | \varphi_{00}, V_0 \stackrel{\text{iid}}{\sim} \mathcal{N}_{k^2}(\varphi_{00}, V_0), \quad h = 1, \dots, H \quad (5)$$

$$\varphi_{00}, V_0 | \varphi_{000}, \lambda, V_{00}, \tau_0 \sim \mathcal{NIW}(\varphi_{000}, \lambda, V_{00}, \tau_0). \quad (6)$$

In (6), $\mathcal{NIW}(\varphi_{000}, \lambda, V_{00}, \tau_0)$ denotes the normal-Inverse Wishart distribution, i.e. $V_0 \sim \mathcal{IW}(\tau_0, V_{00})$ and $\varphi_{00} | V_0 \sim \mathcal{N}(\varphi_{000}, \lambda^{-1}V_0)$, where $\mathcal{IW}(\tau_0, V_{00})$ denotes the inverse-Wishart distribution defined over the space of $k^2 \times k^2$ symmetric and positive definite matrices with mean $V_0/(\tau_0 - k^2 - 1)$.

Posterior inference is performed through a Gibbs sampler algorithm, as detailed in Appendix B. However, it is worth noting that the full-conditional of the weights parameters $\{\boldsymbol{\alpha}_h\}$ in Equation (3) can be derived in closed-form with the introduction of auxiliary variables, using results in Polson et al. (2013) and Rigon and Durante (2021). The full conditional distributions of \mathbf{b} and $\boldsymbol{\gamma}$ are derived as in a standard multivariate Bayesian linear regression models. The full conditionals of the atoms $\{\Phi_{0h}\}$ in the stick-breaking prior (2) are given in the blocked Gibbs sampling of Ishwaran and James (2001).

The code has been implemented in C++ and linked to Python via pybind11 (Jakob et al., 2017).

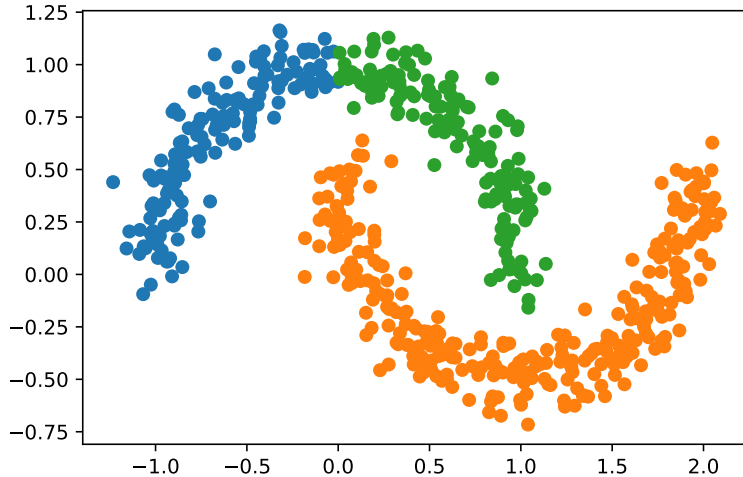


Figure 4: Fixed time covariates for scenario (II)

4 Simulation study

We now present a simulation study to compare the performance of the proposed ‘approach in (2)-(3) versus a similar model but assuming the Φ_i ’s to be generated as independent and identically distributed from a Dirichlet Process (DP, Ferguson, 1973) which is arguably the most popular Bayesian nonparametric prior. (see, e.g. Müller et al., 2015).

We consider three different simulation scenarios. In scenarios (I) and (II) the responses are simulated from (1), while in scenario (III) we simulate each ε_{itj} in $\boldsymbol{\varepsilon}_{it} = (\varepsilon_{it1}, \dots, \varepsilon_{itk})$ from a student-t distribution with mean 0 and 5 degrees of freedom, so that our model is then misspecified. Of course, other kind of misspecifications are possible, for instance, we could generate data from an autoregressive process with a larger lag, but this would lead to much poorer results for any model with our likelihood. For all scenarios, we simulate $N = 300$ independent trajectories $\mathbf{y}_i = (\mathbf{y}_{i1}, \dots, \mathbf{y}_{iT_i})$, with $T_i = 10$ for all i , assuming each \mathbf{y}_{it} to be a three-dimensional vector (i.e., $k = 3$). Moreover, we always set $B = \mathbf{0}$, $\Gamma = 0$ in the data generating process.

In all the scenarios, for each item i , we simulate Φ_i from a discrete mixture, $\Phi_i \stackrel{\text{iid}}{\sim} \sum_{j=1}^3 \pi_j \delta_{\bar{\phi}_j}$, where the $\bar{\phi}_j$ ’s are given in (7) (see here below). Then, conditionally to Φ_i we generate the time-homogeneous covariate vector \mathbf{z}_i . In scenarios (I) and (III) the weights (π_1, π_2, π_3) are set equal to $(0.5, 0.5, 0)$, $\mathbf{z}_i \mid \Phi_i = \bar{\phi}_1 \sim \mathcal{N}_2((-3, -3), I_2)$ and $\mathbf{z}_i \mid \Phi_i = \bar{\phi}_2 \sim \mathcal{N}_2((3, 3), I_2)$

$$\bar{\phi}_1 = \begin{bmatrix} 1.1, 0.0, 0.0 \\ 0.0, 1.1, 0.0 \\ 0.0, 0.0, 1.0 \end{bmatrix}, \quad \bar{\phi}_2 = \begin{bmatrix} 1.1, -0.1, 1.0 \\ -0.1, 1.1, -0.1 \\ 0.0, 0.0, 0.9 \end{bmatrix}, \quad \bar{\phi}_3 = \begin{bmatrix} 0.9, -0.1, 0.0 \\ -0.1, 1.1, -0.1 \\ -0.1, 0.0, 1.5 \end{bmatrix}, \quad (7)$$

while in scenario (II) the weights are $(0.25, 0.25, 0.5)$ and the simulated time-homogeneous covariates are reported in Figure 4. Observe that while in scenario (I) and (III) the covariates in the different clusters are clearly separable, this is no longer the case in scenario (II). Finally, in scenarios (I) and (II) we fix $\Sigma = 0.25I$ in (1), while in scenario (III) the error terms are generated from a student-t distribution as previously explained.

In the simulations, we set the hyperparameters in (6) as follows: $\Phi_{000} = 0$, $\lambda = 0.1$, $V_{00} = I_9$, $\tau_0 = 11$. Moreover, we fix $\Sigma_0 = I_3/\nu$ and $\nu = 5$ (see (4)), so that Σ^{-1} has prior mean equal to I_3 . For our model, we further assume $\mu_\alpha = \mathbf{0}$, $\Sigma_\alpha = I_9$, $\Sigma_B = I_2$ and $\Sigma_\Gamma = I_{18}$; see (3)-(4). For the alternative Dirichlet process prior on the Φ_i ’s, we consider the truncated stick-breaking

	Scenario (I)		Scenario (II)		Scenario (III)	
	LSB	DP	LSB	DP	LSB	DP
OOS	7.5 ± 6.6	65.41 ± 58.8	5.8 ± 3.3	41.9 ± 23.5	91 ± 141	623 ± 1604
INS	3.45 ± 3.12	3.43 ± 3.02	3.9 ± 8.4	4.0 ± 8.5	60.7 ± 114	60.4 ± 113
ARI	1.0	1.0	0.98	0.9	1.0	1.0

Table 1: Simulated dataset: out-of-sample (OOS) and in sample (INS) mean squared prediction errors and Adjuster Rand Index (ARI) for our model (LSB) and the Dirichlet Process prior for Φ_i 's parameters (DP).

approximation (Ishwaran and James, 2001), with total mass parameter equal to 1. For both priors the number of atoms H is set equal to 25.

We assess predictive performance of both models through out-of-sample prediction and l -steps ahead in-sample prediction for observed samples. In the first case (later referred to as OOS), for all scenarios, we generate a new test set of size 300 following the same data generating process outlined above, while in the second experiment (INS) we randomly pick 100 of the 300 trajectories generated and "truncate" them at $T = 5$. In the first setting, the goal is to predict the whole time trajectory given responses at time 1.

We expect our model under prior (2)-(3) to perform much better than when Φ_i are iid from the Dirichlet process, since our model can assign data to clusters based on their time-homogeneous covariates, while the DP prior does not. In the second setting, the goal is to predict $l = 5$ steps in the future, i.e. predict $\mathbf{y}_{i6}, \dots, \mathbf{y}_{i10}$, for the 100 truncated trajectories. Observe that in this case, we condition on the cluster membership inferred through the MCMC simulation, so that the fixed time covariates are not used to assign trajectories to clusters. As such, we expect the DP prior to have better predictive performance than our model since the number of parameters is considerably smaller compared to our model. Finally, we also consider the quality of the estimated random partition of the subjects/datapoints, by computing the Adjusted Rand Index (Hubert and Arabie, 1985) between the point estimate of the partition, obtained by minimizing the Binder loss function with equal missclassification cost (see, e.g., Lau and Green, 2007), based on the MCMC samples and the true partition given by the data generating process.

Goodness-of-fit indices shown in Table 1 confirm our expectations for the out-of-sample testing setting(OOS), that is the proposed approach (denoted in the table as LSB, *logit stick-breaking*) outperforms the DP prior in terms of mean squared prediction. It is clear that for the in-sample predictions both models performs similarly. Note that our model has a slightly better accuracy in terms of clustering for setting (II). This is likely due to the fact that clustering estimation is based also on covariate information and not only on response patterns. The posterior distribution from the DP model favours a larger number of clusters to better approximate the heavy tails of the error's distribution.

Figure 5 shows posterior predictive distributions for both priors under comparison, considering both out-of-sample and in-sample predictions for scenario (I). We can see that in the OOS case the credible bands for the DP prior are very wide, while those under our model are much narrower. Further, in the INS case, both models display better predictive performance and narrower credible bands.

Finally, we simulate a new dataset under scenario (I), but fixing $\bar{\phi}_2 = \mathbf{0}$ so that the corresponding trajectories are well separated; we note that there is no substantial difference in posterior inference. Figure 6 reports kernel density estimates from the MCMC sample of the predictive distribution of Φ_i for scenario (I), for three new observations with time-homogeneous

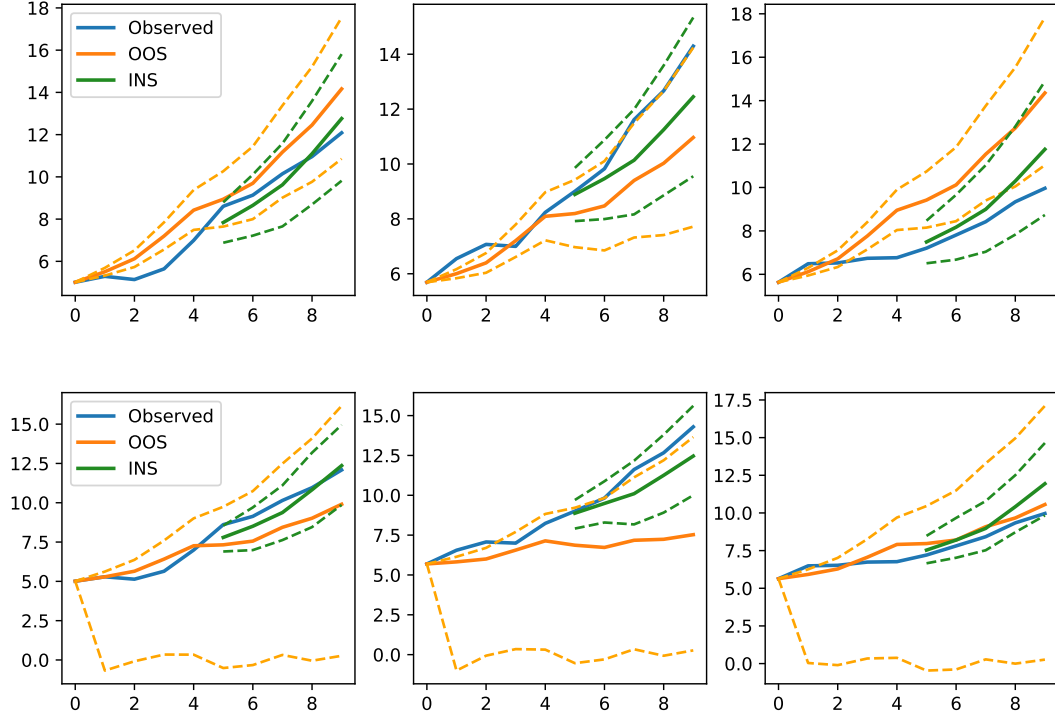


Figure 5: Posterior predictive distributions for both priors under comparison, considering both out-of-sample and in-sample predictions for scenario (I). We show predictive density estimates and credible intervals using our model (top row) and the DP prior (bottom row) for a new subject i . In each panel, the solid blue lines denote the observed trajectory. The OOS prediction (i.e. given \mathbf{z}_i and \mathbf{y}_{i1}) is shown in orange, while the INS prediction (i.e. given \mathbf{y}_{i5} and the cluster label c_i) is shown in green. Solid lines correspond to the median for each time while dashed lines correspond to 95% credible bands of the predictive distributions.

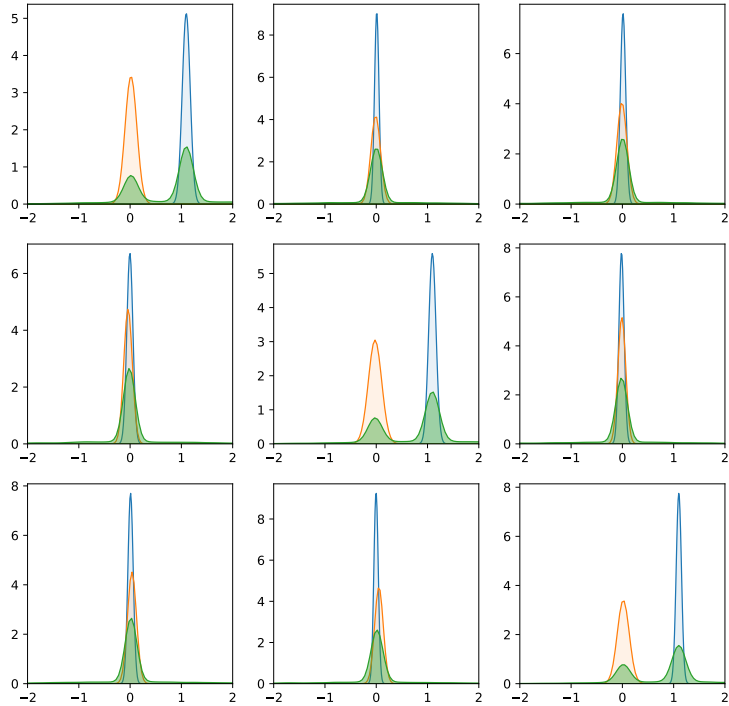


Figure 6: Predictive distributions of Φ_i^{new} corresponding to three subjects with fixed-time covariates equal to $(-3, 0)$ (blue) $(3, 0)$ (orange) and $(0, 0)$ (green), respectively.

covariates equal to $(-3, 0)$, $(3, 0)$ (which coincide with the means of the first and the second group of simulated data) and $(0, 0)$ respectively. Note that the predictive distribution associated to covariate vector equal to $(0, 0)$ (reported in green in Figure 6) is bimodal, giving almost equal mass to values near $\bar{\phi}_1$ and $\bar{\phi}_2$.

This simulation study shows that the proposed models based on a covariate dependent prior outperforms non-dependent alternative prior in terms of prediction. Moreover, also in terms of clustering structure recovery, the covariate dependent prior gives better estimates in case of heavy tail data.

5 Child Growth data

In this section we present posterior results for the Child Growth dataset, detailing prior specification (Section 5.1) and inference in Section 5.2/

5.1 Prior elicitation

Given the complexity of the model and the high-dimensionality of the dataset, prior elicitation needs to be carefully considered. Preliminary analysis shows that that when the variances of the α_h 's (see (3)) or of the atoms Φ_{0h} 's (see (5)) in the logit stick-breaking are large, then all the observations tend to be assigned to the same component. Moreover, the missing data

simulation step has a strong impact on posterior inference. In particular, when using the vague prior described above, in the initial iterations of the MCMC algorithm, typically large missing values were imputed (e.g. 10^5) since both Σ and $\{\Phi_{0h}\}$ would take on unusually large values. Consequently, sampled values for all the other parameters are affected, leading to a poor fit. Hence the use of an uninformative prior is not advisable, causing poor mixing and slow convergence of the chain. Moreover, this is a common situation in complex hierarchical models when non-informative priors are adopted in lower levels.

As such, we opt for informative priors. To set the hyperparameters in the hierarchical marginal prior in (5)-(6), we first obtain the maximum likelihood estimator from a vector autoregressive model:

$$\mathbf{y}_{it} \mid \mathbf{y}_{it-1} \sim \mathcal{N}(\Phi \mathbf{y}_{it-1}, \Sigma), \quad t = 1, \dots, T-1, i = 1, \dots, N \quad (8)$$

which corresponds to (1) when B and Γ are set to zero (their prior expected value) and $H = 1$. We fit (8) using only subjects with no missing responses. Let $\hat{\Phi}$, $\hat{\Sigma}$ denote the maximum likelihood estimator for Φ and Σ respectively. We fix $\Phi_{000} = \hat{\Phi}$, $\lambda = 1$, and select (V_{00}, τ) in (6) so that $\mathbb{E}[V_0] = I$ and $\text{Var}[\{V_0\}_{ii}] = 1.5$. Similarly, we fix Σ_0 and ν in (4) so that $\mathbb{E}[\Sigma] = \hat{\Sigma}$ and $\text{Var}[\{\Sigma_{ii}\}] = 10$. The variance hyperparameter Σ_α in (3) also has an important effect on posterior inference. To set this quantity, we look at the prior distribution of the number of clusters (i.e. *occupied components*) and of the size of the largest cluster. To this end, we perform Monte Carlo simulations. Specifically, we fix the number of components H in the stick-breaking prior equal to 50, set $\Sigma_\alpha = \sigma_\alpha^2 I$, and simulate $\alpha_1, \dots, \alpha_{H-1}$ from (3) with $\mu_\alpha = \mathbf{0}$. Then, for each of the $N = 766$ subjects, we compute the associated weights $\mathbf{w}(\mathbf{z}_i)$ from the logit stick-breaking process, using observed covariates \mathbf{z}_i , and allocate each subject to one of the H components with probability given by the weights $\mathbf{w}(\mathbf{z}_i)$. The above procedure is repeated independently for $M = 10,000$ iterations and we record the number of clusters and the size of the largest cluster. Figure 7 shows the distributions obtained from the Monte Carlo simulation. As σ_α^2 increases, the number of clusters shrinks to 1 and the size of the largest cluster increases accordingly. Hence, we fix $\sigma_\alpha^2 = 5$ so that a priori we should expect approximately 4 – 7 clusters. Finally, we assume $\mu_\alpha = \mathbf{0}$, $\Sigma_B = I_2$ and $\Sigma_\Gamma = I_{18}$ (see (4)); recall that all continuous covariates are standardized.

5.2 Posterior inference results

We apply the model described in Section 3 to the Child growth dataset with hyperparameters set as in Section 5.1. We run the MCMC algorithm for 100,000 iterations, discarding the first 50,000 as burn-in and thinning every 10 iterations, obtaining a final sample size of 5,000 iterations.

Figure 8 shows the posterior distribution of the number of clusters, i.e. of *occupied* parametric components, that is clearly centered around 10-12 clusters. However, interpreting these as the “number of distinct profiles” in the \mathbf{y} ’s may be misleading. Recall that we have specified a covariate-dependent prior for the random partition of patients. Indeed, some clusters can be essentially identical when looking at the response trajectories but different when looking at the covariates. As a point estimate of the latent partition, we choose the one that minimises the Binder loss function under equal misspecification costs (Binder, 1978). The estimated partition consists of seven clusters, of which only four contain least 15 observations. In Figure 9 we display the response trajectories clustered according to the estimated partition. Note that the fourth cluster (bottom row) consists of subjects with at most three visits, except for one single subject with four visits. For this reason, we do not discuss this cluster. Figure 9 shows the time

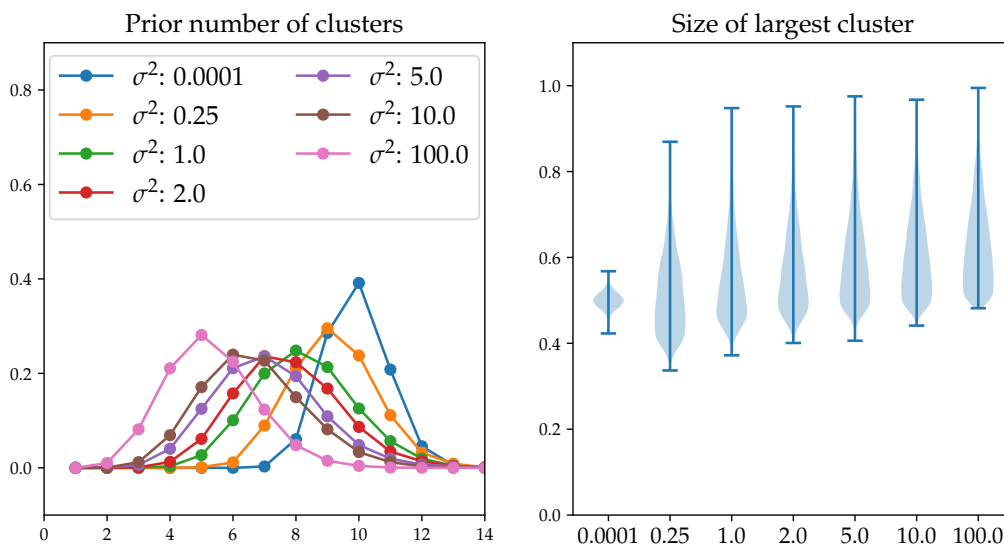


Figure 7: Prior distribution of the number of clusters (left panel) and of the size of the largest cluster as percentage of the whole dataset (right panel), for different values of σ_α .

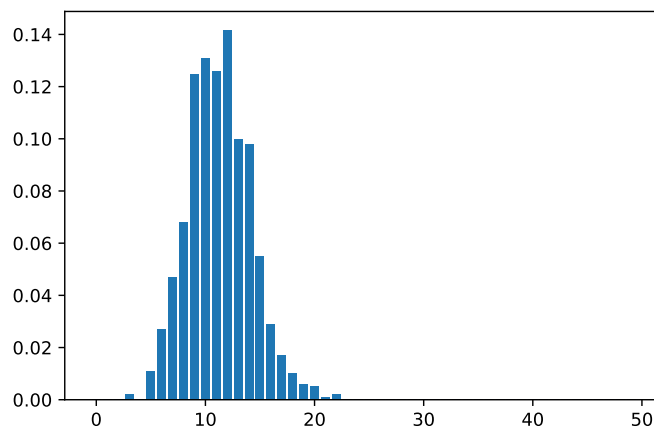


Figure 8: Child Growth dataset: posterior distribution of the number of clusters.

trajectories for patients' height (first column), weight (second column) and BMI. The third row in Figure 9 shows that this cluster contains children with lower weight, and consequently lower BMI than the other two clusters.

As already mentioned, the main three clusters could differ either in the responses or in the covariates (or both). To better understand what discriminates the three main clusters, we perform homogeneity tests for the equality in distribution of both responses and covariates in the different clusters. The results should be considered as a descriptive tool. In particular, for the responses we consider the data on both height and weight at each visit separately and test the equality of the distributions for each pair of clusters. For each of the covariates, we test the equality of their distributions in each possible pair of clusters. For the response variables and continuous covariates, we employ the Kolmogorov-Smirnov (KS) test for equality in distribution and the Pearson's chi-squared test of homogeneity for the categorical covariates. Table 2 reports the p-values associated to the KS test for the responses, while Figure 10 shows the cluster specific empirical distribution of the covariates. From Table 2 and Figure 10, it is

clear that clusters 2 and 3 (second and third rows in Figure 9, respectively) are similar in terms of both responses at each time point. However, Figure 10 (bottom row) suggests that the three main clusters cannot be *explained* only in terms of *ethnicity*, even though cluster 3 contains almost exclusively Chinese children.

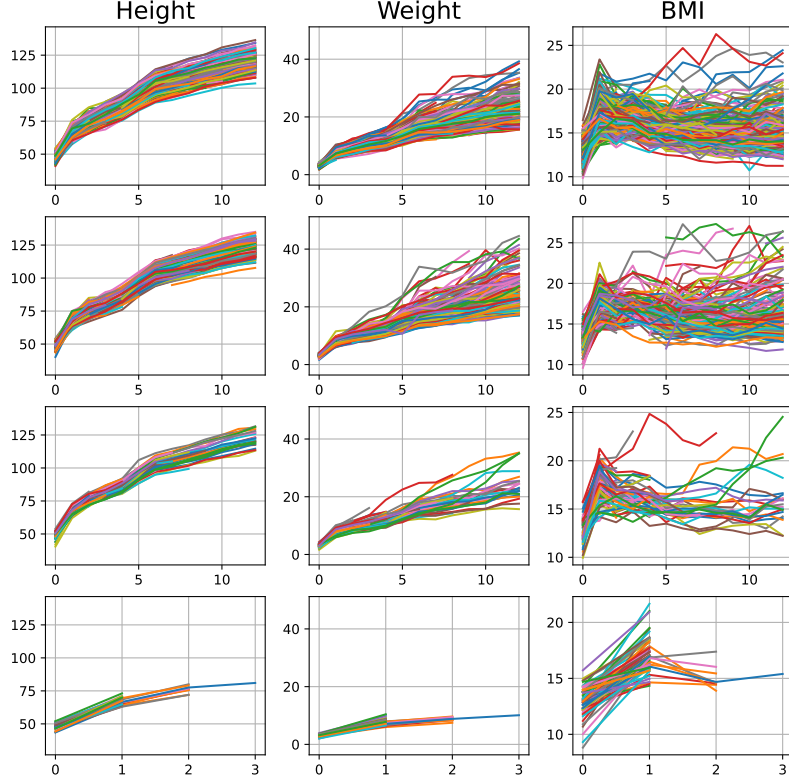


Figure 9: Subject trajectories of height (first column), weight (second column) and BMI (third column) by estimated cluster (by row). The figure reports only the four largest clusters out of the seven estimated.

Next we consider the two parameters in B , i.e. the regression parameters for the square root of time t for the two responses; see (1). The posterior means are 5.55, 0.96, respectively, with marginal standard deviations 0.02, 0.01, thus indicating a non-negligible growth trend for both height and weight, as expected. Figure 11 displays posterior credible intervals for all the parameters in Γ defined in (1), that is the regression coefficients corresponding to the time-homogeneous covariates. The reference group for the categorical covariates has been set such that the baseline level is for a Chinese female child; see Section 2.2. Covariates such as *OGTT 2h*, *ppBMI*, the interaction between education and age, ethnicity (Malay) and the interaction between sex and ethnicity have the strongest effects on height. On the other hand, *parity*, *OGTT 2h*, *ppBMI*, the interaction between education and age (but only the second level of education) and the interaction between sex and ethnicity have a strong association with weight. It is clear from Figure 11 that most of the posterior mass for the marginal distribution of *ethnicity* is concentrated on positive values. Correcting for the autoregressive effect, we see that *ethnicity* might impact obesity as Indian and Malay children are characterised by a larger

Clusters	Height			Weight		
	(1, 2)	(1, 3)	(2, 3)	(1, 2)	(1, 3)	(2, 3)
$t = 1$	0.023	0.000	0.025	0.002	0.296	0.606
$t = 2$	0.000	0.023	0.999	0.000	0.000	0.785
$t = 3$	0.000	0.003	0.797	0.000	0.013	0.815
$t = 4$	0.000	0.000	0.000	0.000	0.253	0.620
$t = 5$	0.046	0.004	0.044	0.000	0.197	0.386
$t = 6$	0.000	0.051	0.701	0.000	0.241	0.254
$t = 7$	0.003	0.113	0.878	0.000	0.431	0.375
$t = 8$	0.000	0.072	0.733	0.000	0.210	0.718
$t = 9$	0.000	0.106	0.984	0.000	0.196	0.715
$t = 10$	0.000	0.112	0.869	0.000	0.341	0.717
$t = 11$	0.000	0.213	0.726	0.000	0.244	0.854
$t = 12$	0.000	0.165	0.877	0.000	0.125	0.932
$t = 13$	0.000	0.179	0.993	0.000	0.042	0.811

Table 2: P-values of the homogeneity tests for the equality in distribution at every visit for each pair of clusters, considering height and weight. Bold numbers correspond to p-values lower than 5%

posterior expected weight, combined in some cases with a lower posterior expected height. Moreover, also correcting for the autoregressive effect, our analysis shows that the posterior expected height of a Chinese male child is larger than the reference (Chinese female child). Similar comments can be made, for instance, regarding Indian male children being smaller than Indian female children, and so on.

Mother’s age and gestational age do not have a strong effect on the child’s height and weight, though this might be due to the fact that these variables are associated with ethnicity; see Figure 2. It is known from the literature that increasing parity is associated with increasing neonatal adiposity in Asian and Western populations (see Tint et al., 2016); this is confirmed by the marginal posterior distribution of the parameter corresponding to the effect of *parity* on weight in Figure 11.

The covariates \mathbf{z}_i ’s play also a key role in the definition of the stick-breaking prior as seen from (3). To assess if the proposed covariate-driven stick-breaking prior provides significant advantages over more standard models, we compare it with three possible competitors. The first one is the parametric version of our model obtained by setting $H = 1$. The second model assumes a truncated Dirichlet process as a prior for Φ_i ’s, with $H = 50$, similarly to what is done in Section 4. Moreover, as third competitor prior, we assume that the Φ_i ’s take into account information from the time-homogeneous covariates through the atoms Φ_{0h} ’s. Specifically, the prior for Φ is specified as in (2), but for each $h = 1, \dots, H$ we define a matrix $\Omega_h \in \mathbb{R}^{k^2 \times q}$ and we let $\text{vec}(\Phi_{0h}(\mathbf{z}_i)) =: \varphi_{0h}(\mathbf{z}_i) = \Omega_h \mathbf{z}_i$. The weights \mathbf{w} in (2) do not depend on the value of \mathbf{z}_i (i.e., $w_h(\mathbf{z}_i) = w_h$) and follow a truncated Dirichlet process prior with $H = 50$. This model can be seen as a finite dimensional approximation of the Linear-DPP in De Iorio et al. (2004).

For all the models, we match the prior for B , Γ , Σ and, when possible also H and the marginal prior distribution of Φ_{0h} . For the Linear-DPP we assume that the vectorization of the Ω_h ’s are independent and identically distributed multivariate Gaussian random variables with mean zero and identity covariance matrix. Since the full conditional distribution of the Ω_h ’s in the case of the Linear-DPP prior does not belong to a known parametric family, we update them via an adaptive Metropolis Hastings (Andrieu and Thoms, 2008) step.

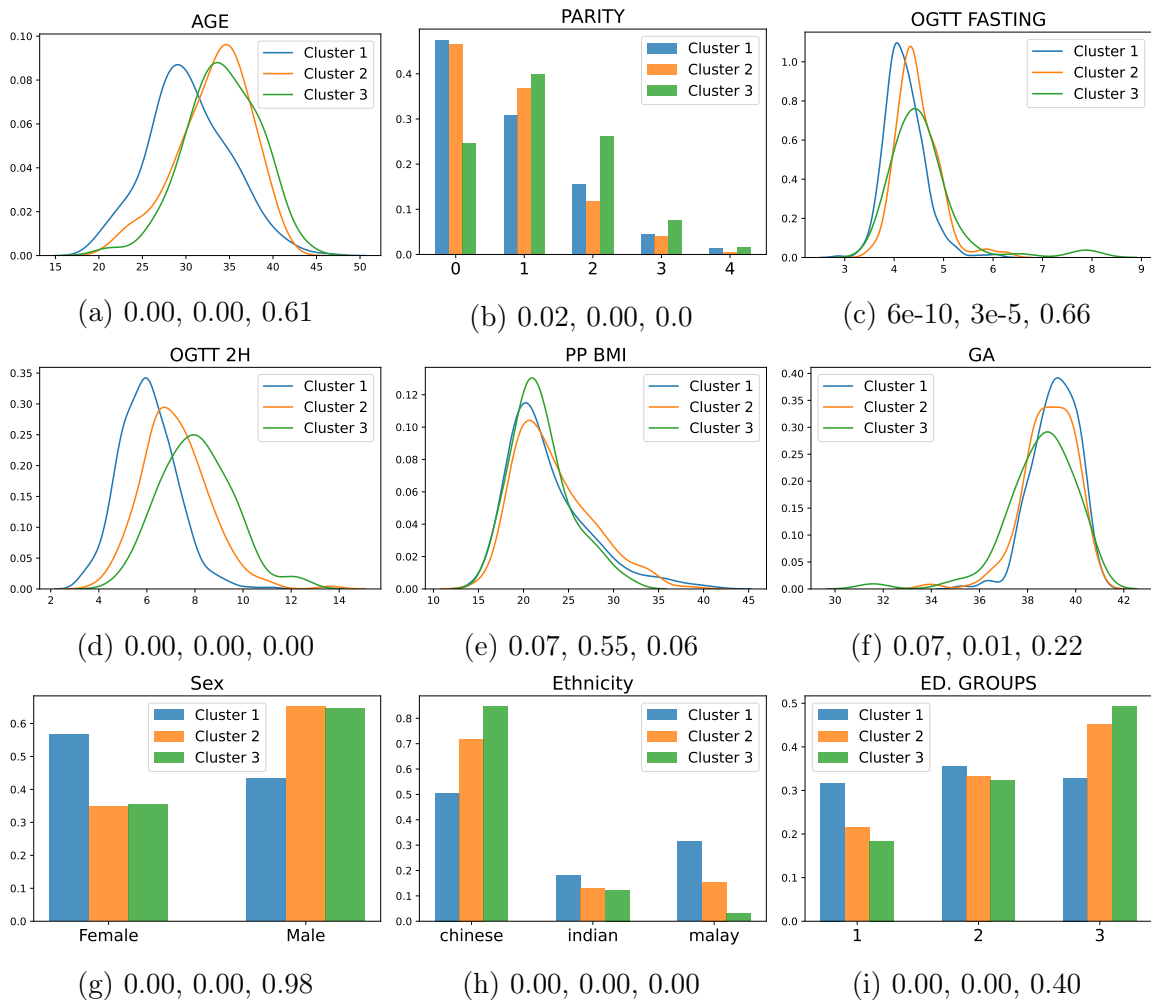


Figure 10: Empirical distribution of the covariates in each cluster. The three numbers below each plot represent the p-values for the homogeneity tests for covariates in clusters (1, 2), (1, 3) and (2, 3), respectively.

The different models are compared using widely applicable information criterion (WAIC, Watanabe, 2013). Higher values of WAIC correspond to better predictive performances. We marginalize the missing values from the predictive distribution of the response trajectory and consider just the marginal predictive distribution for the non-missing values. We found that WAIC is equal to -3.4×10^6 for the Linear-DDP, -6.7×10^5 for the parametric model, -3.9×10^5 for the DP model and -3.4×10^5 for our model, confirming that our model performs better than the competitors. Moreover, we report that the MCMC algorithm for the Linear-DDP requires a much larger number of burn-in iterations (10^5 vs. 10^4) than the other models to reach satisfactory convergence, and that the expected number of cluster a posteriori in the Linear-DPP is around 42. It is then clear that (i) assuming linear dependence of the fixed-time covariates in the autoregressive parameters matrices Φ_i does not give good predictive fit (or at least not better than our model), and that (ii) adding covariate information in the stick-breaking prior improves the prediction performance.

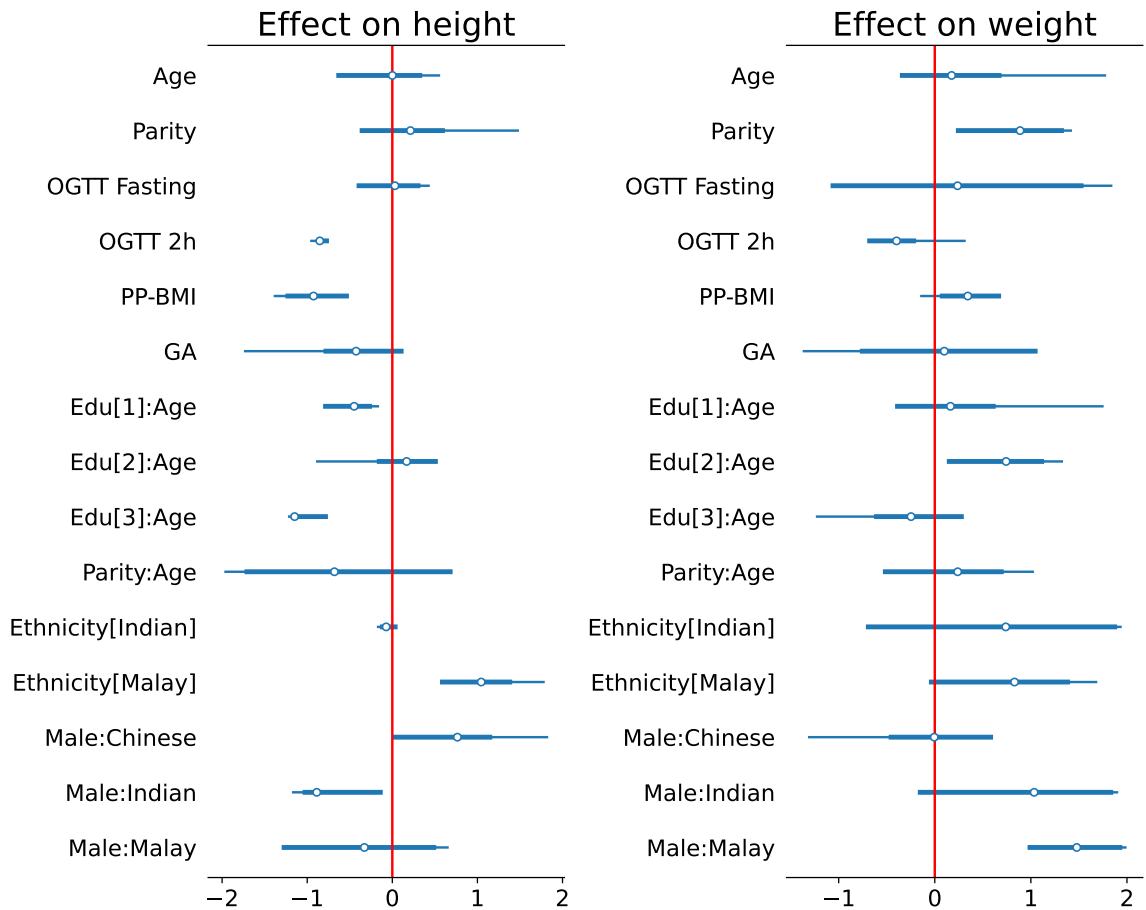


Figure 11: Posterior credible intervals of the regression coefficients in Γ for the height (left plot) and weight of the children (right plot). Thin lines correspond to 95% credible intervals, while thick lines to 80% credible intervals.

6 Summary

The aim of this manuscript is to cluster children according to obesity growth patterns. Obesity is an epidemic, increasingly affecting children. Overweight or obesity in childhood may be critical as they often persist into adulthood due to both physiological and behavioral factors.

Motivation for our study stems from a child growth dataset. To analyze these data we developed a Bayesian nonparametric VAR joint model for height and weight profiles for these children. One key aspect behind the modeling choice was to cluster the corresponding joint time-evolving profiles using the available covariate information. The model features a logit stick-breaking construction that can accommodate covariate dependence in the mixture weights. This allows us to relate certain baseline conditions of these children, such as sex or ethnicity, to obesity patterns. Ethnic differences in obesity are of interest as they could be due to genetic factors, dietary intake, cultural or socioeconomic factors. The analysis allowed us to identify important clusters of children that are characterized by differences in the trajectories or in the covariates or both.

Posterior inference was carried out by means of an efficient posterior simulation that exploits recently developed results on logit stick-breaking priors, which facilitates postulating covariate dependence in the mixture weights. For this implementation we chose to fix a sufficiently large number of components from which we focused on the number of these that were actually

occupied (we referred to these as *clusters*). The results obtained were compared against competitor models, and we found that our approach provides superior performance as measured by standard quantities such as the WAIC.

Acknowledgments

This work was partially funded by grant FONDECYT 1180034.

A Further plots

We show the scatterplots of the responses (height and weight) at time $t = 0, 1, 2$ versus all continuous covariates at the baseline of the dataset on obesity for Children in Singapore. When the covariate we consider is discrete, scatterplots are replaced by boxplots. The left column of Figure 12 reports scatterplots or boxplots of the height at time $t = 0$, while the left column of Figure 13 reports similar plots for the weight at time $t = 0$. The central and right columns of Figures 12 and 13 display the same plots of the responses at time $t = 1$ and 2.

B The Gibbs sampler

Posterior inference for our logit stick-breaking model (1)- (6) is carried out using a Gibbs sampler algorithm, with full conditionals outlined below. The joint distribution of data and parameters is described here

$$\begin{aligned} \mathcal{L}(\mathbf{Y}_1, \dots, \mathbf{Y}_N, B, \Gamma, \Sigma, \Phi_1, \dots, \Phi_N) &= \prod_{i=1}^N \mathcal{L}(Y_{i1}, \dots, Y_{iT_i} | \mathbf{b}, \boldsymbol{\gamma}, \Sigma, \Phi_1, \dots, \Phi_n) \\ &\times \pi(\mathbf{b}) \times \pi(\boldsymbol{\gamma}) \times \pi(\Sigma) \times \pi(\Phi_1, \dots, \Phi_N | \mathbf{z}_1, \dots, \mathbf{z}_N) \end{aligned} \quad (9)$$

In what follows, "rest" refers to the data and all parameters except for the one to the left of "|". Moreover we adopt the matrix notation or the vector one for all parameters interchangeably.

As in Ishwaran and James (2001), to sample from the stick-breaking prior on Φ_i , as it is standard, we use cluster indicator latent variables, that will be indicated by G_i .

1. The full-conditional for the parameters $\mathbf{b} = \text{vec}(B)$ can be obtained by noticing that using the following change of variable

$$\mathbf{y}_{it} - \Phi_i \mathbf{y}_{it-1} - \Gamma \mathbf{z}_i = B \mathbf{x}_{it} + \boldsymbol{\epsilon}_{it}$$

we recover the standard expression of Bayesian multivariate linear regression, let $\mathbf{w}_{it} = \mathbf{y}_{it} - \Phi_i \mathbf{y}_{it-1} - \Gamma \mathbf{z}_i$. We have:

$$\mathbf{w}_{it} = \mathbf{x}_{it}^T B^T + \boldsymbol{\epsilon}_{it}.$$

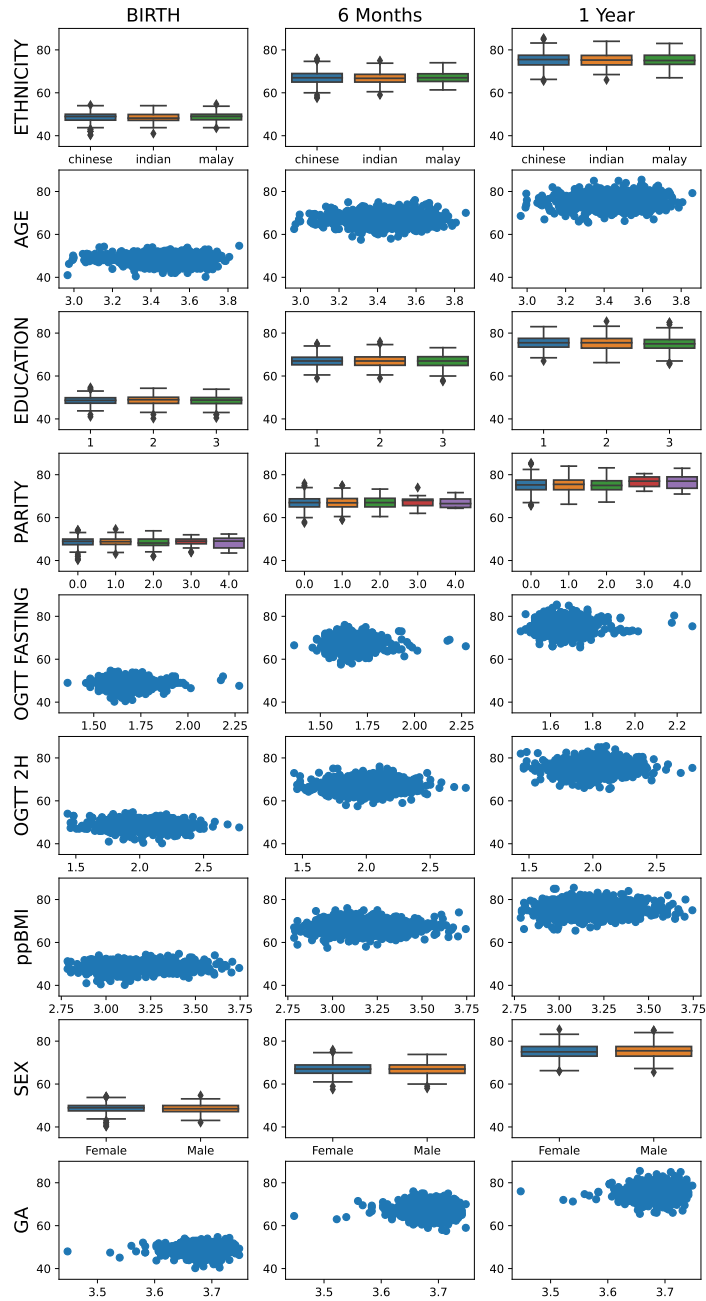


Figure 12: Scatterplots of covariates against the height at birth (left column), at six months of age (center) and at one year of age (right column).

Using standard techniques, calling

$$\mathbf{W} = \begin{bmatrix} \mathbf{w}_{1,1} \\ \vdots \\ \mathbf{w}_{i,T_1} \\ \vdots \\ \mathbf{w}_{N,1} \\ \vdots \\ \mathbf{w}_{N,T_N} \end{bmatrix} \quad \mathbf{X} = \begin{bmatrix} \mathbf{x}_{1,1} \\ \vdots \\ \mathbf{x}_{1,T_1} \\ \vdots \\ \mathbf{x}_{N,1} \\ \vdots \\ \mathbf{x}_{N,T_N} \end{bmatrix}$$

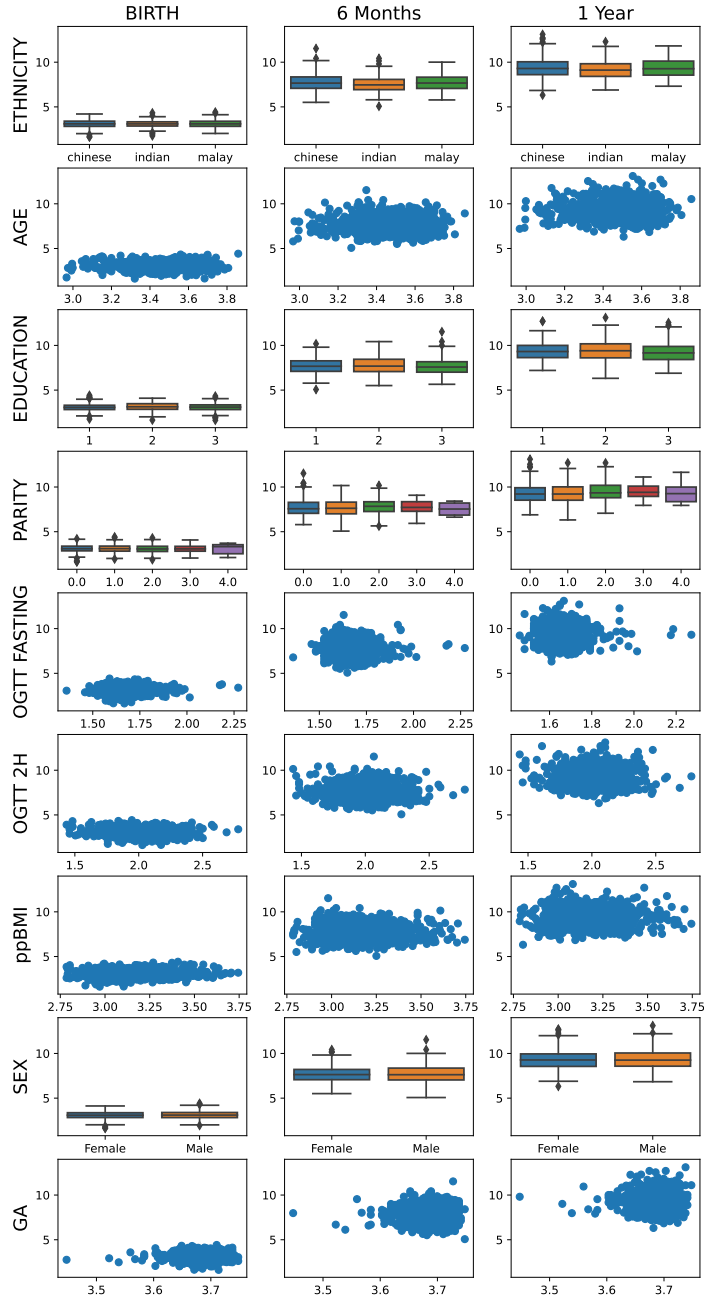


Figure 13: Scatterplots of covariates against the weight at birth (left column), at six months of age (center) and at one year of age (right column).

We can write the system in vector form as:

$$\mathbf{W} = \mathbf{X}\mathbf{B}^T + \mathbf{E},$$

where \mathbf{W}, \mathbf{E} are $[\sum_{i=1}^N T_i \times k]$ matrices and \mathbf{X} is $[\sum_{i=1}^N T_i \times p]$. By standard multivariate regression theory we have that

$$\begin{aligned} \mathbf{b} | \mathbf{X}, \mathbf{W}, \Sigma &\sim \mathcal{N}(\tilde{\mu}_b, \tilde{\Sigma}_b) \\ \mu_b &= (\Sigma^{-1} \otimes \mathbf{X}^T \mathbf{X} + \Sigma_b^{-1})^{-1} \left((\Sigma^{-1} \otimes \mathbf{X}^T \mathbf{X}) \hat{\beta} + \Sigma_b^{-1} \tilde{\beta}_0 \right) \\ \tilde{\Sigma}_b &= \Sigma^{-1} \otimes \mathbf{X}^T \mathbf{X} + \Sigma_b^{-1}, \end{aligned}$$

where $\hat{\beta}$ is the standard frequentist estimate:

$$\hat{\beta} = (X^T X)^{-1} X^T \mathbf{W}.$$

We thus obtain:

$$\mathcal{L}(\mathbf{b}|\text{rest}) = \mathcal{N}(\tilde{\mu}_b, \tilde{\Sigma}_b) \quad (10)$$

2. Analogously to what we did in the previous step, the law of γ can be deduced from standard Bayesian multivariate regression theory after a suitable change of variable:

$$\mathbf{y}_{it} - \Phi_i \mathbf{y}_{it-1} - B \mathbf{x}_{it} = \Gamma \mathbf{z}_i + \boldsymbol{\epsilon}_{it}$$

We thus recover the same equations as in the previous section.

3. To sample from $\mathcal{L}(\Sigma|\text{rest})$ we analyze the full conditional (to simplify the notation we impose $\mathbf{y}_{i0} = \mathbf{0}$ for all i 's):

$$\begin{aligned} \mathcal{L}(\Sigma^{-1}|-) &\propto \prod_{i=1}^N \prod_{t=1}^{T_i} \frac{1}{|2\pi\Sigma|^{\frac{1}{2}}} \exp\left(-\frac{1}{2}(\mathbf{y}_{it} - \Phi_i \mathbf{y}_{it-1} - B \mathbf{x}_{it} - \Gamma \mathbf{z}_i)^T \Sigma^{-1} (\mathbf{y}_{it} - \Phi_i \mathbf{y}_{it-1} - B \mathbf{x}_{it} - \Gamma \mathbf{z}_i)\right) \\ &\quad \times \frac{|\Sigma_0|^{\frac{\tau}{2}}}{2^{\frac{\tau k}{2}} \Gamma_k\left(\frac{\tau}{2}\right)} |\Sigma|^{-\frac{\tau+k+1}{2}} \exp\left(-\frac{1}{2} \text{tr}(\Sigma_0 \Sigma^{-1})\right) \\ &\propto \frac{|\Sigma|^{-\frac{\tau+k+1}{2}}}{|2\pi\Sigma|^{\frac{1}{2}} \prod_{i=1}^N \prod_{t=1}^{T_i}} \exp\left(-\frac{1}{2} E\right). \end{aligned}$$

By using the trace trick, circularity of the trace and linearity of the trace operator we get that

$$E = \text{tr} \left(\left(\sum_{i=1}^N \sum_{t=1}^{T_i} (\mathbf{y}_{it} - \Phi_i \mathbf{y}_{it-1} - B \mathbf{x}_{it} - \Gamma \mathbf{z}_i)(\mathbf{y}_{it} - \Phi_i \mathbf{y}_{it-1} - B \mathbf{x}_{it} - \Gamma \mathbf{z}_i)^T + \Sigma_0 \right) \Sigma^{-1} \right).$$

We can deduce that $\mathcal{L}(\Sigma | \text{rest}) = IW(\tilde{\nu}, \tilde{\Sigma}_0)$ with parameters

$$\begin{aligned} \tilde{\nu} &= \nu + \sum_{i=1}^N T_i \\ \tilde{\Sigma}_0 &= \sum_{i=1}^N \sum_{t=1}^{T_i} (\mathbf{y}_{it} - \Phi_i \mathbf{y}_{it-1} - B \mathbf{x}_{it} - \Gamma \mathbf{z}_i)(\mathbf{y}_{it} - \Phi_i \mathbf{y}_{it-1} - B \mathbf{x}_{it} - \Gamma \mathbf{z}_i)^T + \Sigma_0. \end{aligned} \quad (11)$$

4. The component indicator variables are sampled considering the usual change of variables

$$\mathbf{w}_{it} = \Phi_i(\mathbf{z}_i) \mathbf{y}_{it-1} + \boldsymbol{\epsilon}_{it},$$

where $\mathbf{w}_{it} = \mathbf{y}_{it} - B \mathbf{x}_{it} - \Gamma \mathbf{z}_i$. We have that:

$$\begin{aligned} P(G_i = h | \text{rest}) &\propto P(G_i = h) f(\mathbf{w}_{i1}, \dots, \mathbf{w}_{iT_i} | G_i = h) \\ &\propto P(G_i = h) \times f(\mathbf{w}_{i1} | G_i = h, \text{rest}) \prod_{t=2}^{T_i} f(\mathbf{w}_{it} | \mathbf{y}_{it-1}, \text{rest}) \\ &\propto \nu_h(\mathbf{z}_i) \prod_{l=1}^{h-1} (1 - \nu_l(\mathbf{z}_i)) \times \mathcal{N}(\mathbf{w}_{i1}; B \mathbf{x}_{i1} + \Gamma \mathbf{z}_i, \Sigma) \prod_{t=2}^{T_i} \mathcal{N}(\mathbf{w}_{it}; \Phi_{0h} \mathbf{y}_{it-1} B \mathbf{x}_{it} + \Gamma \mathbf{z}_i, \Sigma). \end{aligned} \quad (12)$$

Thus the conditional distribution of G_i is a discrete distribution with weights as in (12).

5. For each cluster-specific Φ_{0h} we have that, for the i 's such that $G_i = h$:

$$\mathbf{y}_{it} = \Phi_{0h}\mathbf{y}_{it-1} + Bx_{it} + \Gamma z_i + \epsilon_{it}.$$

Defining:

$$\mathbf{Y} = \begin{bmatrix} \mathbf{y}_{11} - B\mathbf{x}_{11} - \Gamma z_1 \\ \vdots \\ \mathbf{y}_{1T_1} - B\mathbf{x}_{1T_1} - \Gamma z_1 \\ \vdots \\ \mathbf{y}_{N_i1} - B\mathbf{x}_{N_i1} - \Gamma z_{N_i} \\ \vdots \\ \mathbf{y}_{N_iT_{N_i}} - B\mathbf{x}_{N_iT_{N_i}} - \Gamma z_{N_i} \end{bmatrix} \quad X = \begin{bmatrix} \mathbf{y}_{10} \\ \vdots \\ \mathbf{y}_{1T_1-1} \\ \vdots \\ \mathbf{y}_{N_i1} \\ \vdots \\ \mathbf{y}_{N_iT_i-1} \end{bmatrix}$$

where the \mathbf{y}_i s have been selected such that they belong to cluster h , we have the following Seemingly Unrelated Representation:

$$\mathbf{Y} = X\Phi_{0h}^T + E. \quad (13)$$

Thus, we can recover the full conditional for $\varphi_{0h} := \text{vec}(\Phi_{0h})$ using standard Bayesian multivariate regression theory. In particular we have that:

$$\begin{aligned} \varphi_{0h}|Y, X, \Sigma &\sim \mathcal{N}(\mu_{0h}, \Sigma_{0h}) \\ \Sigma_{0h} &= \Sigma^{-1} \otimes X^T X + V_0^{-1} \\ \mu_{0h} &= \Sigma_{0h}^{-1} ((\Sigma^{-1} \otimes X^T X)\widehat{\varphi_{0h}} + V_0^{-1}\varphi_{00}), \end{aligned} \quad (14)$$

where $\widehat{\varphi_{0h}} = (X^T X)^{-1}X^T Y$ is the frequentist estimation.

6. Since the update of α_h is independent of the AR model, we can simply refer to Rigon and Durante (2021) where a latent variable ω_{ih} is introduced. Defining $\rho_{ih}|\mathbf{z}_i \sim \mathcal{B}(\nu_h(\mathbf{z}_i))$, the couple (ω_{ih}, ρ_{ih}) is updated as in Polson et al. (2013) from a Pólya-Gamma distribution.
7. As the joint law does not depend from the parameters Φ_{00}, V_0 except for the prior specification of Φ_{0h} , we can update them using a Normal-Normal-inverse-Wishart scheme as follows:

$$\begin{aligned} \varphi_{0h}|\varphi_{00}, V_0 &\stackrel{\text{iid}}{\sim} \mathcal{N}(\varphi_{00}, V_0) \\ \varphi_{00}|\varphi_{000}, V_0, \lambda_0 &\sim \mathcal{N}\left(\varphi_{000}, \frac{1}{\lambda_0}V_0\right) \\ V_0|\varphi_{00}, \tau_0 &\sim \mathcal{IW}(V_{00}, \nu_0), \end{aligned} \quad (15)$$

From this we have that:

$$\begin{aligned} \varphi_{00}|V_0, \varphi_{01}, \dots, \varphi_{0H} &\sim \mathcal{N}\left(\frac{H\bar{\varphi}_0 + \lambda\varphi_{000}}{H + \lambda}, \frac{1}{H + \lambda}V_0\right) \\ V_0|\varphi_{01}, \dots, \varphi_{0H} &\sim \mathcal{IW}\left(V_{00} + HS + \frac{H\lambda}{H + \lambda}(\bar{\varphi}_0 - \varphi_{000})(\bar{\varphi}_0 - \varphi_{000})^T, H + \nu_0\right) \\ \bar{\varphi}_0 &= \frac{1}{H} \sum_{h=1}^H \varphi_{0h} \end{aligned} \quad (16)$$

$$S = \frac{1}{H} \sum_{h=1}^H (\varphi_{0h} - \bar{\varphi}_0)(\Phi_{0h} - \bar{\varphi}_0)^T$$

An iteration of our Gibbs samples consists in sampling from the full conditionals described in steps 1. through 7. above, iteratively. Moreover, if there are missing responses as in the case of the application, at each iteration, before step 1., we sample the missing responses from their full conditional as described below.

B.1 Sampling missing responses

We start by deriving the joint law of the vector $\mathbf{y}_i = (\mathbf{y}_{i1}, \dots, \mathbf{y}_{iT_i})$, given Φ_i, B, Γ and Σ . Consider the simplified VAR model, for a single patient (we drop the index i).

$$\mathbf{y}_1 = \epsilon_1, \quad \mathbf{y}_t | X_{t-1} = \Phi \mathbf{y}_{t-1} + \epsilon_t. \quad (17)$$

By expressing the joint law as $\mathcal{L}(\mathbf{y}_1, \dots, \mathbf{y}_T) = \mathcal{L}(\mathbf{y}_1) \mathcal{L}(\mathbf{y}_2 | \mathbf{y}_1) \dots \mathcal{L}(\mathbf{y}_T | \mathbf{y}_{T-1})$ and through some basic linear algebra, we can derive that the vectorization of $(\mathbf{y}_1, \dots, \mathbf{y}_T)$ is a jointly normal random vector with zero mean. The precision matrix $\tilde{\Sigma}^{-1}$ of the normal distribution has a blocked structure made of $T \times T$ blocks, each of which is an $r \times r$ matrix. The (i, j) -th block equals to:

$$\tilde{\Sigma}_{i,j}^{-1} = \begin{cases} (I + \Phi)^T \Sigma^{-1} (I + \Phi), & \text{if } i = j < T \\ \Sigma^{-1}, & \text{if } i = j = T \\ \Phi^T \Sigma^{-1}, & \text{if } |i - j| = 1 \\ 0 & \text{if } |i - j| > 1 \end{cases} \quad (18)$$

Going back to the full model, it is easy to see that with a change of variable $\mathbf{y}_{it} \mapsto \mathbf{y}_{i,t} - B\mathbf{x}_{i,t} - \Gamma z_i$ we recover the same VAR system in (17). Hence, the vectorization of \mathbf{y}_i follows a multivariate normal with precision matrix given by (18) and mean $\boldsymbol{\mu}$ given by the vectorization of $(B\mathbf{x}_{i1} + \Gamma z_i, \dots, B\mathbf{x}_{iT_i} + \Gamma z_i)$.

To simulate missing values in \mathbf{y}_i , we exploit the joint law derived above and the fact that the conditional distributions of entries in a Gaussian random vector are available in close form. In particular, if there are k missing values in \mathbf{y}_i , we first apply a permutation matrix P to the vectorization of \mathbf{y}_i so that the missing entries are the first k (this will in turn change the mean $\boldsymbol{\mu}$ to $P\boldsymbol{\mu}$ and the covariance matrix to $P^T \tilde{\Sigma} P$). Then, using notation $\mathbf{x}^{:k}$ and $\mathbf{x}^{k:}$ for the first k elements of vector \mathbf{x} and the elements $k+1, \dots$ respectively, and notation $A^{:k,\ell}$ for a matrix A analogously, where the first index denotes the rows and the second index denotes the columns, we have that:

$$(P\mathbf{y}_i)^{:k} | (P\mathbf{y}_i)^{k:} \sim \mathcal{N}_k(\bar{\boldsymbol{\mu}}, \bar{\Sigma}),$$

where

$$\bar{\boldsymbol{\mu}} = [P(B\mathbf{x}_i + \Gamma z_i)]^{:k} + [P^T \tilde{\Sigma} P]^{k:,k} \left([P^T \tilde{\Sigma} P]^{:k,:k} \right)^{-1} (P\mathbf{y}_i^{k:} - P(B\mathbf{x}_i + \Gamma z_i)^{k:})$$

and

$$\bar{\Sigma} = [P^T \tilde{\Sigma} P]^{k:,k} \left([P^T \tilde{\Sigma} P]^{:k,:k} \right)^{-1} [P^T \tilde{\Sigma} P]^{:k,k:}$$

See Proposition 3.13 in Eaton (1983) for a proof.

References

- Andrieu, C. and Thoms, J. (2008). “A tutorial on adaptive MCMC.” *Statistics and computing*, 18(4), 343–373.
- Argiento, R. and De Iorio, M. (2019). “Is infinity that far? A Bayesian nonparametric perspective of finite mixture models.” *arXiv preprint arXiv:1904.09733*.
- Billio, M., Casarin, R., and Rossini, L. (2019). “Bayesian nonparametric sparse VAR models.” *Journal of Econometrics*, 212(1), 97–115.
- Binder, D. A. (1978). “Bayesian cluster analysis.” *Biometrika*, 65(1), 31–38.
- Canova, F. and Ciccarelli, M. (2004). “Forecasting and turning point predictions in a Bayesian panel VAR model.” *Journal of Econometrics*, 120(2), 327–359.
- Catalano, P., Drago, N., and Amini, S. (1995). “Factors affecting fetal growth and body composition.” *Am J Obstet Gynecol.*, 172(5), 1459–63.
- CDS (2018). “Centers for Disease Control and Prevention - Behavior, environment, and genetic factors all have a role in causing people to be overweight and obese.” Accessed: 19-01-2018. URL <https://www.cdc.gov/genomics/resources/diseases/obesity/index.htm>
- Chung, Y. and Dunson, D. B. (2009). “Nonparametric Bayes conditional distribution modeling with variable selection.” *Journal of the American Statistical Association*, 104(488), 1646–1660.
- Crevaschi, A., De Iorio, M., Kothandaraman, N., Yap, F., Tint, M. T., and Eriksson, J. (2021). “Integrating metabolic networks and growth biomarkers to unveil potential mechanisms of obesity.” *arXiv preprint arXiv:2111.06212*.
- Daniels, M. J. and Pourahmadi, M. (2002). “Bayesian analysis of covariance matrices and dynamic models for longitudinal data.” *Biometrika*, 89(3), 553–566.
- De Iorio, M., Müller, P., Rosner, G. L., and MacEachern, S. N. (2004). “An ANOVA model for dependent random measures.” *Journal of the American Statistical Association*, 99(465), 205–215.
- Després, J.-P., Lemieux, I., Bergeron, J., Pibarot, P., Mathieu, P., Larose, E., Rodés-Cabau, J., Bertrand, O. F., and Poirier, P. (2008). “Abdominal Obesity and the Metabolic Syndrome: Contribution to Global Cardiometabolic Risk.” *Arteriosclerosis, Thrombosis, and Vascular Biology*, 28(6), 1039–1049.
- Eaton, M. L. (1983). “Multivariate statistics: a vector space approach.” *John Wiley & Sons, Inc., New York*.
- Ferguson, T. S. (1973). “A Bayesian analysis of some nonparametric problems.” *Ann. Statist.*, 1, 209–230.
- Fields, D., Krishnan, S., and Wisniewski, A. (2009). “Sex differences in body composition early in life.” *Gend Med.*, 6(2), 369–75.

- Fox, C. S., Massaro, J. M., Hoffmann, U., Pou, K. M., Maurovich-Horvat, P., Liu, C.-Y., Vasan, R. S., Murabito, J. M., Meigs, J. B., Cupples, L. A., D’Agostino, R. B., and O’Donnell, C. J. (2007). “Abdominal Visceral and Subcutaneous Adipose Tissue Compartments.” *Circulation*, 116(1), 39–48.
- Frühwirth-Schnatter, S. and Malsiner-Walli, G. (2019). “From here to infinity: sparse finite versus Dirichlet process mixtures in model-based clustering.” *Advances in data analysis and classification*, 13(1), 33–64.
- Gao, F., Zheng, K. I., Wang, X.-B., Sun, Q.-F., Pan, K.-H., Wang, T.-Y., Chen, Y.-P., Targher, G., Byrne, C. D., George, J., et al. (2020). “Obesity is a risk factor for greater COVID-19 severity.” *Diabetes care*, 43(7), e72–e74.
- Godfrey, K. M., Haugen, G., Kiserud, T., Inskip, H. M., Cooper, C., Harvey, N. C. W., Crozier, S. R., Robinson, S. M., Davies, L., the Southampton Women’s Survey Study Group, and Hanson, M. A. (2012). “Fetal Liver Blood Flow Distribution: Role in Human Developmental Strategy to Prioritize Fat Deposition versus Brain Development.” *PLOS ONE*, 7(8), 1–7.
- Hales, C. M., Fryar, C. D., Carroll, M. D., Freedman, D. S., and Ogden, C. L. (2018). “Trends in obesity and severe obesity prevalence in US youth and adults by sex and age, 2007-2008 to 2015-2016.” *Jama*, 319(16), 1723–1725.
- Hubert, L. and Arabie, P. (1985). “Comparing partitions.” *Journal of classification*, 2(1), 193–218.
- Ishwaran, H. and James, L. F. (2001). “Gibbs sampling methods for stick-breaking priors.” *Journal of the American Statistical Association*, 96(453), 161–173.
- Jakob, W., Rhinelander, J., and Moldovan, D. (2017). “pybind11 – Seamless operability between C++11 and Python.” <https://github.com/pybind/pybind11>.
- Joshi, N., Kulkarni, S., Yajnik, C., Joglekar, C., Rao, S., Coyaji, K., H.G., L., Rege, S., and Fall, C. (2005). “Increasing maternal parity predicts neonatal adiposity: Pune Maternal Nutrition Study.” *Am J Obstet Gynecol*, Sep;193(3 Pt 1), 783–9.
- Kalli, M. and Griffin, J. E. (2018). “Bayesian nonparametric vector autoregressive models.” *Journal of econometrics*, 203(2), 267–282.
- Kundu, S. and Lukemire, J. (2021). “Non-parametric Bayesian Vector Autoregression using Multi-subject Data.” *arXiv preprint arXiv:2111.08743*.
- Lau, J. W. and Green, P. J. (2007). “Bayesian model-based clustering procedures.” *Journal of Computational and Graphical Statistics*, 16(3), 526–558.
- MacEachern, S. N. (2000). “Dependent dirichlet processes.” *Unpublished manuscript, Department of Statistics, The Ohio State University*, 1–40.
- Misra, A. and Khurana, L. (2011). “Obesity-related non-communicable diseases: South Asians vs White Caucasians.” *International journal of obesity*, 35(2), 167–187.
- Müller, P., Quintana, F., and Rosner, G. L. (2011). “A product partition model with regression on covariates.” *Journal of Computational and Graphical Statistics*, 20(1), 260–278.

- Müller, P., Quintana, F. A., Jara, A., and Hanson, T. (2015). *Bayesian nonparametric data analysis*. Springer Series in Statistics. Springer, Cham.
- Nightingale, C. M., Rudnicka, A. R., Owen, C. G., Cook, D. G., and Whincup, P. H. (2010). “Patterns of body size and adiposity among UK children of South Asian, black African–Caribbean and white European origin: Child Heart And health Study in England (CHASE Study).” *International Journal of Epidemiology*, 40(1), 33–44.
- Park, J.-H. and Dunson, D. B. (2010). “Bayesian generalized product partition model.” *Statistica Sinica*, 1203–1226.
- Pi-Sunyer, X. (2009). “The medical risks of obesity.” *Postgraduate medicine*, 121(6), 21–33.
- Polson, N. G., Scott, J. G., and Windle, J. (2013). “Bayesian Inference for Logistic Models Using Pólya-Gamma Latent Variables.” *Journal of the American Statistical Association*, 108(504), 1339–1349.
- Qasim, A., Turcotte, M., De Souza, R., Samaan, M., Champredon, D., Dushoff, J., Speakman, J., and Meyre, D. (2018). “On the origin of obesity: identifying the biological, environmental and cultural drivers of genetic risk among human populations.” *Obesity reviews*, 19(2), 121–149.
- Quintana, F. A., Mueller, P., Jara, A., and MacEachern, S. N. (2022). “The dependent Dirichlet process and related models.” *Statistical Science*, 37(1), 24–41.
- Ren, L., Du, L., Carin, L., and Dunson, D. B. (2011). “Logistic stick-breaking process.” *Journal of Machine Learning Research*, 12(1).
- Rigon, T. and Durante, D. (2021). “Tractable Bayesian density regression via logit stick-breaking priors.” *Journal of Statistical Planning and Inference*, 211, 131–142.
- Rodríguez, A. and Dunson, D. B. (2011). “Nonparametric Bayesian models through probit stick-breaking processes.” *Bayesian Anal.*, 6(1), 145–177.
URL <https://doi.org/10.1214/11-BA605>
- Rodríguez, G., Samper, M. P., Ventura, P., Moreno, L. A., Olivares, J. L., and Pérez-González, J. M. (2004). “Gender differences in newborn subcutaneous fat distribution.” *European journal of pediatrics*, 163(8), 457–461.
- Simon, L., Borrego, P., Darmaun, D., Legrand, A., Rozé, J., and Chauty-Fronidas, A. (2013). “Effect of sex and gestational age on neonatal body composition.” *Br J Nutr.*, 109(6), 1105–8.
- Soh, S.-E., Tint, M. T., Gluckman, P. D., Godfrey, K. M., Rifkin-Graboi, A., Chan, Y. H., Stünkel, W., Holbrook, J. D., Kwek, K., Chong, Y.-S., et al. (2014). “Cohort profile: Growing Up in Singapore Towards healthy Outcomes (GUSTO) birth cohort study.” *International journal of epidemiology*, 43(5), 1401–1409.
- Symonds, M., Mendez, M., Meltzer, H., Koletzko, B., Godfrey, K., Forsyth, S., and van der Beek, E. (2013). “Early Life Nutritional Programming of Obesity: Mother-Child Cohort Studies.” *Ann Nutr Metab*, 62(2), 137–145.

- Tint, M. T., Fortier, M. V., Godfrey, K. M., Shuter, B., Kapur, J., Rajadurai, V. S., Agarwal, P., Chinnadurai, A., Niduvaje, K., Chan, Y.-H., et al. (2016). “Abdominal adipose tissue compartments vary with ethnicity in Asian neonates: Growing Up in Singapore Toward Healthy Outcomes birth cohort study.” *The American journal of clinical nutrition*, 103(5), 1311–1317.
- Watanabe, S. (2013). “A widely applicable Bayesian information criterion.” *Journal of Machine Learning Research*, 14(Mar), 867–897.
- Whincup, P. H., Gilg, J. A., Owen, C. G., Odoki, K., Alberti, K. G. M. M., and Cook, D. G. (2005). “British South Asians aged 13–16 years have higher fasting glucose and insulin levels than Europeans.” *Diabetic Medicine*, 22(9), 1275–1277.
- WHO (2022). “World Health Organization - Obesity and overweight.” Accessed: 11-01-2022. URL <https://www.who.int/news-room/fact-sheets/detail/obesity-and-overweight>
- Yajnik, C. S., Fall, C. H. D., Coyaji, K. J., Hirve, S. S., Rao, S., Barker, D. J. P., Joglekar, C., and Kellingray, S. (2003). “Neonatal anthropometry: the thin–fat Indian baby. The Pune Maternal Nutrition Study.” *International Journal of Obesity*, 27(2), 173–180.
- Yajnik, C. S., Lubree, H. G., Rege, S. S., Naik, S. S., Deshpande, J. A., Deshpande, S. S., Joglekar, C. V., and Yudkin, J. S. (2002). “Adiposity and Hyperinsulinemia in Indians Are Present at Birth.” *The Journal of Clinical Endocrinology & Metabolism*, 87(12), 5575–5580.
- Zhang, T., Whelton, P. K., Xi, B., Krousel-Wood, M., Bazzano, L., He, J., Chen, W., and Li, S. (2019). “Rate of change in body mass index at different ages during childhood and adult obesity risk.” *Pediatric obesity*, 14(7), e12513.